Int. J. Electrochem. Sci., 15 **(2020)** 12329 – 12338, doi: 10.20964/2020.12.40

International Journal of
ELECTROCHEMICAL
SCIENCE
www.electrochemsci.org

Long- term Corrosion Behavior of Low Carbon Steel Bars Embedded in Building Concrete: Effect of Silica Fume and Dolomite Powder as Partial Replacements of Portland Cement

Kangqiang Lin[1], *Tian Zheng*[2,*]

[1] School of Architecture and Applied Art, Guangzhou Academy of Fine Arts, Guangzhou, 510006, China
[2] R&F Group, Guangzhou, 510623, China
[*]E-mail: linkangqiang0101@sina.com, zhengtian0101@sina.com

Received: 3 August 2020 / *Accepted:* 22 September 2020 / *Published:* 31 October 2020

In this study, the incorporating effect of different combinations of silica fume (SF) and dolomite powder (DP) into ordinary Portland cement (OPC) on corrosion behavior of carbon steel reinforced concrete was investigated. Electrochemical impedance spectroscopy (EIS) and polarization analyses in 3.5% NaCl were used to obtain electrochemical corrosion data. Fitting of the EIS data to a suitable equivalent electrical circuit showed that the highest corrosion enhancement was achieved for the mixture with SF (40 kg/m^3) and DP (80 Kg/m^3) in OPC (M4 sample). Polarization measurements also indicated that the M4 sample had the lowest corrosion density, highest corrosion potential with corrosion inhibition efficiency of η= 94%. Consistent results of electrochemical measurements and water absorption show that the mineral admixtures enhance the durability of concrete exposed to corrosive agents by preventing the surface of carbon steel bars from reaching the aggressive ions.

Keywords: Corrosion resistance; Dolomite powder and Silica fume; Electrochemical Impedance spectroscopy; Low carbon steel bars; Polarization

1. INTRODUCTION

Reinforced concrete is used frequently as a structural material in construction due to its high compressive resistance and low cost. However, some aggressive specimens result in degradation of steel reinforcement, cement and concrete [1, 2]. Corrosion of steel bars in reinforced concrete structures has been one of the most important problems. Therefore, many researchers have studied decreasing the steel corrosion rate with different approaches such as using different reinforced steels, using corrosion inhibitors, replacement Portland cement with other materials, the effect of different exposure environments [3-7].

Corrosion protection of embedded steel in concrete is done by two mechanisms, the physical and chemical protection. The chemical protection is provided with high pH solution in the concrete pores which causes steel passivation and also the physical protection is provided with covering of concrete which prevents the surface of steel. Presence of some additives such as fly ash, kiln slag, fibers, rice husk ash and silica fume has shown both of compressive strength and durability of concrete exposed to aggressive agents such as chloride containing environments [8-11]. The other factor should be noticed is the ecological issue. One of the corrosion resistant replacement additives is silica fume. Silica fume (SF) is a by-product of the silicon and ferrosilicon alloy production with contents of amorphous silica. The average particle diameter is about 100 times smaller than that of Portland cement particles. Moreover, its specific surface area is about 300- 13000 m^2/kg, which is extremely large in comparison to that of Portland cement with 300-400 m^2/kg [12-14]. Silica fume reacts in two ways with adding to the fresh concrete. In the pozzolanic reaction, it generally reacts chemically with the calcium hydroxide (CH) producing an additional amount of hydrated calcium silicate (C_S_H), which is responsible for the resistance of the concrete. In addition, it produces a filler effect (micro filler effect) when the mixture pores are filled with very small admixture particles [15]. For these reasons, introducing silica fume to Portland cement can reduce the porosity and increase the strength and durability of concrete [16]. Water can enter by capillary action. Since silica fumes reduce porosity, less water is absorbed into the reinforced concrete with fewer and smaller capillary pores which can be directly associated with improving the corrosion resistance [17]. Dolomite is a carbonate sedimentary rock with a high amount of carbonate in the form of $CaMg(CO_3)_2$, and also with similar mechanical properties to those of limestone. Dolomite is used in the glass, furnaces and manufacturing of steel [18]. It is harder and more available than limestone and can be applied in the fabrication of concrete as a great building material. Kamal *et al* in their study reported that the bond strength of concrete increases with addition of silica fume or fly ash along with dolomite powder as fillers [19, 20].

In this work we investigated the effect of incorporating different combinations of silica fume (SF) and dolomite powder (DP) in the concrete on the corrosion protection of the embedded steel bar. A reinforced concrete made with OPC was used as a control sample. The corrosion behavior of samples was evaluated in 3.5% NaCl solution using open circuit potential (OCP), electrochemical impedance spectroscopy and polarization for 3 months. Morphology of samples was studied by scanning electron microscopy and also water affinity of them with respect to various combinations was also studied.

2. MATERIALS AND METHODS

The chemical compositions of low carbon steel are listed in Table 1. Concrete specimens were prepared with replacement of OPC (M0) with various concentrations of SF and DP by weight of cement.

Table 1. Chemical compositions of carbon steel bars used in this work

Element	**C**	**Si**	**Mn**	**Cr**	**Ni**	**Al**	**Cu**	**Fe**
(wt.%)	0.1	1.5	0.83	0.06	0.1	0.01	0.34	Bal.

The chemical properties of Ordinary Portland cement, silica fume and dolomite powder are described in Table 2. The blend cements were mixed by a high-speed mixer to obtain a homogeneous dispersion. Five mixtures were prepared with DP replacing up to 20% cement weight along with SF which replaced 10% of cement by weight. The compositions of mixes are given in Table 3. Also, the total content of powder (cement+ silica fume+ dolomite powder) was 400 kg/m^3.

Table 2. Chemical composition of Ordinary Portland cement, silica fume, dolomite powder (% by mass)

Composition	Materials		
	Ordinary Portland cement	Silica fume	Dolomite powder
SiO_2	23.3	93.8	0.85
Fe_2O_3	4.67	1.38	0.50
Al_2O_3	4.14	0.41	0.75
CaO	57.26	0.20	28.7
MgO	2.31	0.47	19.3
K_2O	1.02	0.43	---
Na_2O	0.38	0.35	---
SO_3	3.37	0.22	---
CO_2	---	---	45.5
L.O.I	2.10	2.62	44.5

The concrete samples were poured into the PVC pipe cylindrical molds with a diameter of 10 cm and a height of 30 cm for 24 h at 95% relative humidity and room temperature to complete the hydration reaction.

EIS was carried out using a potentiostat (Ivium, De Zaale 11, 5612 AJ Eindhoven, Netherlands) with reference to OCP with a voltage amplitude of 10 mV and in the frequency range of 100 KHz to 0.01 Hz after three months immersion time. A three-electrode cell was applied for the measurements which contain the steel bar embedded in concrete as the working electrode, a platinum wire and a saturated calomel electrode as an auxiliary and a reference electrode, respectively. All analyses were done in the 3.5% w/w NaCl solution. The EIS data were fitted using ZView software by appropriate equivalent electric circuits. The potentiodynamic polarization measurement was carried out with a rate of 1 mV s^{-1} from 0.25 V. The corrosion current density (i_{corr}) and the corrosion potential (E_{corr}) were

obtained from the Tafel extrapolation of polarization curves (50-100 mV away from E_{corr}). According to ASTM C642 water absorption value was determined by drying a sample with a constant mass, and then immersing it in water and measuring the mass of standard surface dry. Water absorption was the proportion of the difference between the two values measured to the dry mass. The surface morphologies of specimens were studied by Zeiss Sigma 300 VP scanning electron microscope.

Table 3. Compositions of prepared mixtures

Sample	Mixture compositions (kg/m^3)					
	Cement	Silica fume	Dolomite powder	Water	Fine aggregates	Coarse aggregates
M0	400	---	---	200	700	1008
M1	360	---	40	200	685	972
M2	360	40	---	200	685	972
M3	320	40	40	200	685	972
M4	280	40	80	200	685	972

3. RESULTS AND DISCUSSION

3.1. Open circuit potential

The open circuit potential (OCP) measurements provide the qualitative information of corrosion [21]. Figure 1 represents the variations of OCP values of the steel bars embedded in different concrete samples in 3.5% NaCl solution. According to ASTM C876 [22], the potential values which are less than -350 mV are in the high risk region and also the ones between -200 mV and -350 mV are in intermediate corrosion risk region. Therefore, the potential values of OPC (M0 mixture) are in the high risk corrosion region for the whole exposure time, which is associated with initiation of pitting corrosion or small rupture of the passive layer [23]. Moreover, the potential values for the concrete containing mineral admixtures oscillate from -310 mV to -235 mV that are at intermediate corrosion risk concerning the corrosion. The protection provided against corrosion may be attributed to the reaction of SF with calcium hydroxide released during the hydration of the cement and produced additional hydrated calcium silicate, which enhances the durability and mechanical properties of the concrete [24]. In addition, the DP can increase the chemical adhesion due to the high surface area which prevents the growth of calcium hydroxide. As we can see in Figure 1, M4 mixture presented more positive potentials and also more stable potential values in comparison with those of other mixtures which may be related to increasing age of concrete with increasing the amount of SF and DP [15].

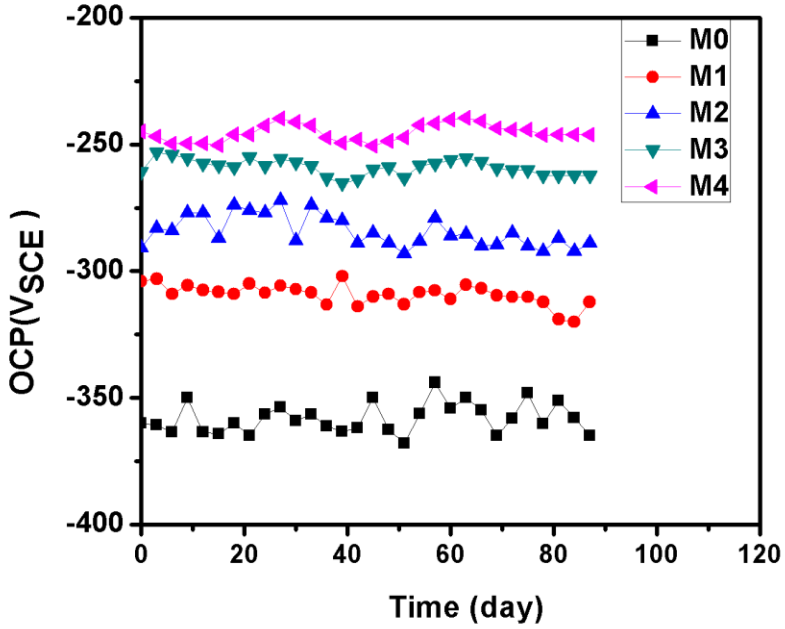

Figure 1. Open circuit potential values of the steel bars embedded in different concrete samples in 3.5% NaCl solution

3.2 Electrochemical impedance spectroscopy

Electrochemical impedance spectroscopy **(**EIS) measurements were done for all samples in 3.5% NaCl solution. The Nyquist and Bode diagrams are shown in Figure 2, respectively corresponding to the carbon steel bars in reinforced concrete prepared without and with different admixtures in 3.5% NaCl solution after three months.

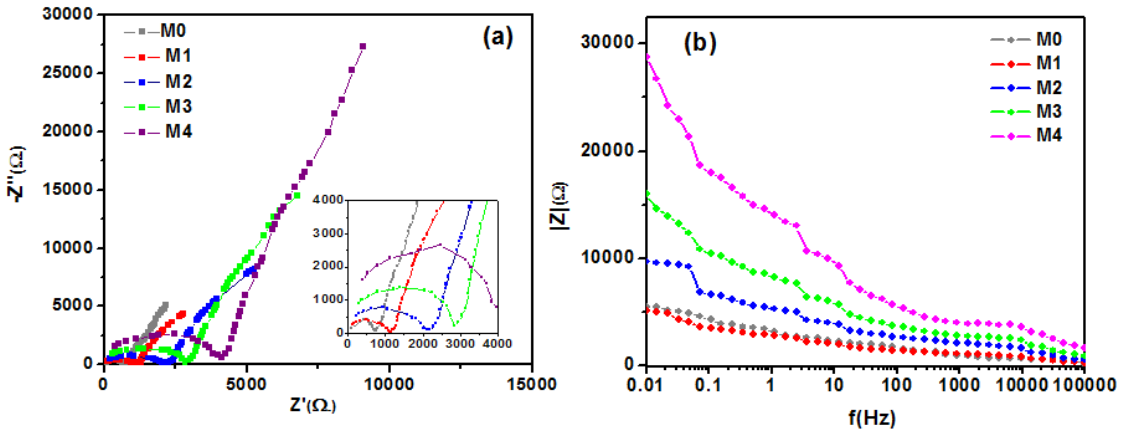

Figure 2. (a) Nyquist and (b) Bode diagrams for carbon steel bars in reinforced concrete prepared without and with different admixtures exposed to 3.5% NaCl solution after three months

The used suitable equivalent circuit is indicated in Figure 3 which R_s is the solution resistance. CPE_c and R_c elements that are parallel to each other are the constant phase element and the resistance

for coated concrete, respectively. R_{ct} is the charge transfer resistance and CPE_{dl} corresponds to the constant phase element of the double layer which is related to the electrostatic accumulation of nonhomogeneous charges near the steel surface that determines the properties and structure of materials [25]. The value of *n* varies between 0 and 1 which depends on factors such as roughness of surface, layer porosity and non-uniform conductivity of layers on the surface [26]. The obtained data are indicated in Table 4.

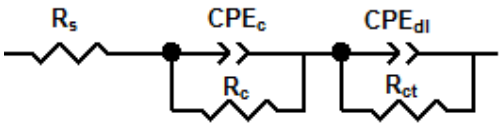

Figure 3. Used electrical equivalent circuit to fit the data from EIS measurement

Table 4. Obtained electrochemical parameters of fitting the Nyquist diagrams for carbon steel bars in reinforced concrete prepared with different admixtures exposed to 3.5% NaCl solution.

Mixtures	$R_s(\Omega)$	$R_c(\Omega)$	CPE_c (μFcm^{-2})	n_c	R_{ct} (Ω)	CPE_{dl}(μFcm^{-2})
M0	64	645	10.4	0.7	4000	7.5
M1	54	1065	9.2	0.73	4692	5.6
M2	50	2066	8.3	0.78	7581	4.3
M3	60	2818	6.1	0.82	12433	2.8
M4	45	5200	4.4	0.87	22700	1.6

The first semicircle in Figure 2a which corresponds to the properties of the concrete has moved to the right (radius size) with increasing the quantity of SF and DP. This reveals the strength increase and a decrease in the capacitance of the concrete simultaneously as it is consistent with EIS results in Table 4. With incorporating the higher amount of DP and SF, the second semicircle which represents the properties of the double layer has also been removed to the right. Thus, R_{ct} increases and CPE_{dl} reduces. In Table 4 it can be seen that specimens with various combinations present the higher corrosion resistance compared to the mixture M0, especially in the case in which the concrete contains SF and the highest amount of DP. As a result of the reaction of silica fume with cement, CSH is produced and also by filling of the concrete pores, permeability of concrete reduces [12]. Furthermore, chloride binding probably increases in samples containing DP due to the formed hydrotalcite [27] and the porosity of the concrete decreases. In addition, the DP can improve the chemical adhesion due to the high surface area which prevents the growth of calcium hydroxide [19]. Therefore, it provides corrosion protection by retarding diffusion of corrosive species to the metal surface. Hence, according to the obtained results all mixtures in terms of corrosion protection could fulfill expectations for structural applications.

3.3 Potentiodynamic polarization

Figure 4 shows the polarization curves obtained from the measurements on carbon steel bars in different concrete samples exposed to 3.5% NaCl solution after three months.

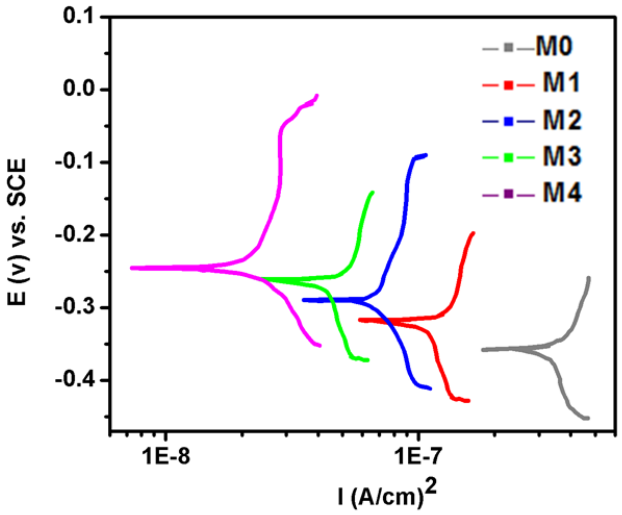

Figure 4. Potentiodynamic polarization of carbon steel embedded in different concrete samples exposed to 3.5% NaCl solution after three months

In Table 5, the values of corrosion potential, corrosion current density, anodic and cathodic Tafel slopes obtained from polarization curves are given. It can be observed that the corrosion potential of steel bars in samples with different combinations of admixtures shows a positive shift relative to M0 mixture which demonstrates a higher corrosion resistance. It can be concluded that the anodic metal dissolution was retarded by varying the concrete content [28]. Clearly, corrosion current densities of steel bars in concrete containing admixtures are lower than that of concrete without them which the lowest value is for the mixture of M4. As mentioned in the EIS section, incorporating SF to the concrete reacts with released calcium hydroxide during the cement hydration and forms extra calcium silicate hydrate, which improves the mechanical properties and the durability [29]. In addition, DP prevents the growth of calcium hydroxide and permeation of aggressive ions by formation of hydrotalcite. The inhibition efficiency η (%) of samples is calculated by Equation 1 where $i_{corr-abs}$ and $i_{corr-pres}$ are the corrosion current density of steel bars in concrete with and without admixtures, respectively [25].

$$\eta(\%) = \frac{i_{corr-abs} - i_{corr-pres}}{i_{corr-abs}} \times 100$$

Obtained values of η in Table 5 indicate that the corrosion of steel bars is inhibited by the addition of admixtures in concrete. When DP is added to the concrete, η =70% and it increases with adding SF to it. Finally, for the mixture of M4 the corrosion inhibition efficiency reaches 94%, which is the highest and consistent with the results of EIS. The values of the cathodic Tafel slopes in Table 5 do not change significantly for the concrete with different combinations of fillers, which implies that

does not affect the cathodic reaction [30, 31]. The variation of the anodic Tafel slopes indicating a blockage at the anodic reaction sites, which affect the anodic mechanism. Enhancing the more corrosion inhibition is done by incorporation of SF and DP into the concrete simultaneously according to the increase in the compressive strength and micro filler effects.

Table 5. Corrosion parameters of steel bars in 3.5% NaCl solution

Mixtures	E_{Corr} (V) vs. SCE)	i_{Corr}(μA/cm^2)	β_a (mV/dec)	-β_c (mV/dec)	η(%)
M0	-0.361	0.332	23	52	---
M1	-0.321	0.097	27	56	70
M2	-0.292	0.065	32	57	80
M3	-0.265	0.040	32	56	87
M4	-0.244	0.018	35	53	94

3.4 Water absorptivity

Figure 5 shows the water absorption of the samples in 3.5 % NaCl solution after 3 months. The average value of three measurements for each sample are given. It shows that SF and DP as mineral admixtures have significant effects on water absorption of samples, which varied between 8.7% and 3.5%. When these admixtures are incorporated in concrete, it can reduce capillaries and large pores. As we can see in Figure 5 less water is absorbed. Mixture of M4 demonstrates the lowest water absorption which can be related to the densest microscopic pore structure and it is not permeable to corrosive species [17]. Density is increased with increasing the amount of DP in concrete due to micro-filler effects which is caused by the fine grained DP [32]. Therefore, the corrosion resistance of steel bars in chloride solution improves.

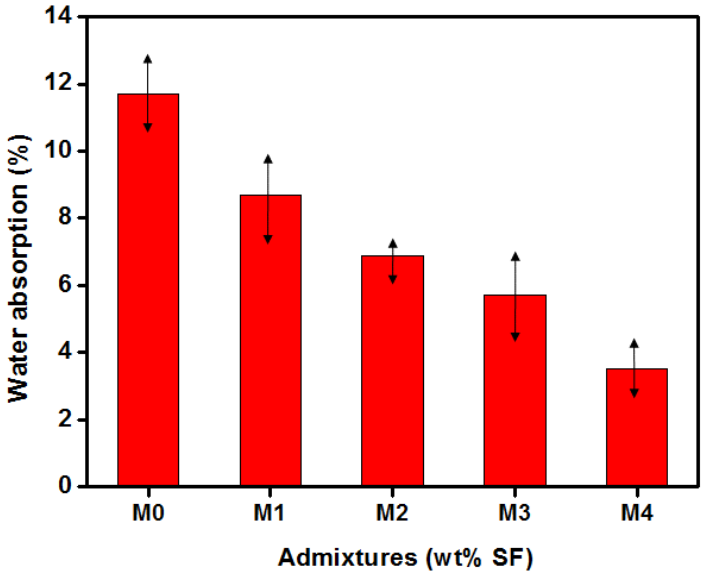

Figure 5. Water absorption of the samples in 3.5 % NaCl solution after 3 months

Figure 6 indicates the surface morphology of carbon steel bars in the mixtures of M0 and M4 exposed to 3.5% NaCl solution after three months, respectively. The surface of the steel bar in the M4 mix is more uniform than that of M0 mix which is consistent with polarization and EIS results. Obtained reinforced concrete is more chemically resistant and also has a lower pores and yields high strength and impermeable concrete.

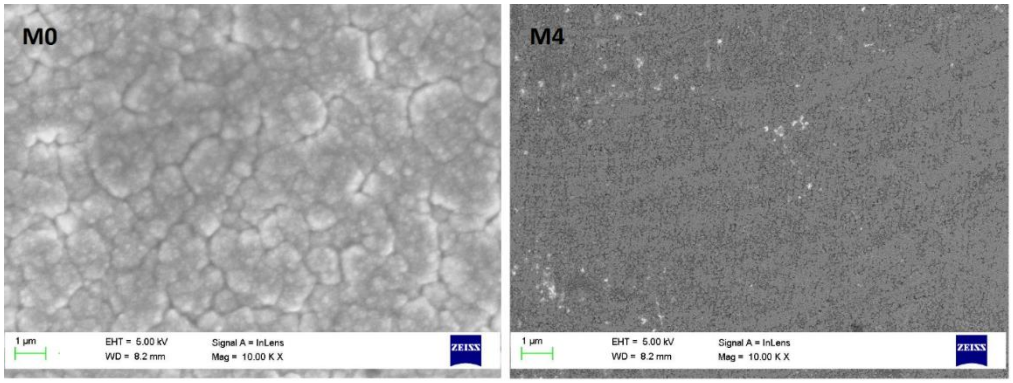

Figure 6. SEM images of carbon steel surface in the concrete with the different combinations, exposed to 3.5% NaCl solution after three months

4. CONCLUSION

The effect of incorporating various combinations of silica fume and dolomite powder into OPC on corrosion behavior of embedded carbon steel bars reinforced concrete in 3.5% NaCl was studied. The EIS results showed that the highest corrosion enhancement is achieved for the mixture of M4 with SF (40 kg/m^3) and DP (80 Kg/m^3) due to the more decrease of water absorptivity and aggressive ions permeability. Polarization measurements also showed that the M4 sample has the lowest corrosion density, highest corrosion potential with a 94% corrosion inhibition efficiency. Consistent results of electrochemical measurements and water absorption indicate that SF and DP as mineral admixtures enhance the durability of concrete and corrosion resistance of steel bars in the concrete exposed to a corrosive environment.

References

1. H.G. Campos Silva, P. Garces Terradillos, E. Zornoza, J.M. Mendoza-Rangel, P. Castro-Borges and C.A. Juarez Alvarado, *Sustainability*, 10 (2018) 2004.
2. J. Rouhi, C.R. Ooi, S. Mahmud and M.R. Mahmood, *Electronic Materials Letters*, 11 (2015) 957.
3. R.E. Melchers and C. Li, *Cement and concrete research*, 39 (2009) 1068.
4. B. Pradhan, *Construction and Building Materials*, 72 (2014) 398.
5. N. San Nicolás de los Garza, *International Journal of Electrochemical Science*, 11 (2016) 10306.

6. G. Santiago Hurtado, *International Journal of Electrochemical Science*, 11 (2016) 4850.
7. M. Alimanesh, J. Rouhi and Z. Hassan, *Ceramics International*, 42 (2016) 5136.
8. H. AzariJafari, M.J.T. Amiri, A. Ashrafian, H. Rasekh, M.J. Barforooshi and J. Berenjian, *Journal of cleaner production*, 223 (2019) 575.
9. R.B. Ardalan, Z.N. Emamzadeh, H. Rasekh, A. Joshaghani and B. Samali, *Journal of Sustainable Cement-Based Materials*, 9 (2020) 1.
10. M. Ghasemi, H. Rasekh, J. Berenjian and H. AzariJafari, *Construction and Building Materials*, 222 (2019) 424.
11. L. Nan, C. Yalan, L. Jixiang, O. Dujuan, D. Wenhui, J. Rouhi and M. Mustapha, *RSC Advances*, 10 (2020) 27923.
12. A. Afshar, S. Jahandari, H. Rasekh, M. Shariati, A. Afshar and A. Shokrgozar, *Construction and Building Materials*, 262 (2020) 120034.
13. J. Rouhi, S. Mahmud, S. Hutagalung and S. Kakooei, *Micro & Nano Letters*, 7 (2012) 325.
14. R. Mohamed, J. Rouhi, M.F. Malek and A.S. Ismail, *International Journal of Electrochemical Science*, 11 (2016) 2197.
15. J. Dotto, A. De Abreu, D. Dal Molin and I. Müller, *Cement and concrete composites*, 26 (2004) 31.
16. K. Ramamurthy, E.K. Nambiar and G.I.S. Ranjani, *Cement and concrete composites*, 31 (2009) 388.
17. J. Hou and D. Chung, *Corrosion Science*, 42 (2000) 1489.
18. C. Sadik, O. Moudden, A. El Bouari and I.-E. El Amrani, *Journal of Asian Ceramic Societies*, 4 (2016) 219.
19. M.M. Kamal, M.A. Safan and M.A. Al-Gazzar, *Advances in concrete construction*, 1 (2013) 273.
20. J. Rouhi, M.R. Mahmood, S. Mahmud and R. Dalvand, *Journal of Solid State Electrochemistry*, 18 (2014) 1695.
21. S. Kakooei, H.M. Akil, A. Dolati and J. Rouhi, *Construction and Building Materials*, 35 (2012) 564.
22. F.G.d. Silva and J.B.L. Liborio, *Materials Research*, 9 (2006) 209.
23. M.A. Baltazar-Zamora, D. M Bastidas, G. Santiago-Hurtado, J.M. Mendoza-Rangel, C. Gaona-Tiburcio, J.M. Bastidas and F. Almeraya-Calderón, *Materials*, 12 (2019) 4007.
24. N. Amudhavalli and J. Mathew, *International Journal of Engineering Sciences & Emerging Technologies*, 3 (2012) 28.
25. H.S. Bahari and H. Savaloni, *Metals and Materials International*, (2019) 1.
26. H.S. Bahari and H. Savaloni, *Materials Research Express*, 6 (2019) 086570.
27. A. Machner, M. Zajac, M.B. Haha, K.O. Kjellsen, M.R. Geiker and K. De Weerdt, *Cement and Concrete Research*, 107 (2018) 163.
28. W.Z. Shengpin Liu, *International Journal of Electrochemical Science*, 15 (2020) 3825.
29. Y. Zhou, S. Xu, L. Guo, S. Zhang, H. Lu, Y. Gong and F. Gao, *RSC Advances*, 5 (2015) 14804.
30. A. Ansari, M. Znini, I. Hamdani, L. Majidi, A. Bouyanzer and B. Hammouti, *J. Mater. Environ. Sci*, 5 (2014) 81.
31. J. Rouhi, S. Kakooei, M.C. Ismail, R. Karimzadeh and M.R. Mahmood, *International Journal of Electrochemical Science*, 12 (2017) 9933.
32. S. Barbhuiya, *Construction and Building Materials*, 25 (2011) 3301.